Desalination and Water Treatment
www.deswater.com
doi: 10.5004/dwt.2022.28353

254 (2022) 287–301
April

Removal of Methylene blue from aqueous solution with activated carbon produced from hazelnut shells by K_2CO_3 activation

Birsen Sarıci[a], Sukru Karatas[b,*], Esra Altintig[c]

[a]*Department of Nutrition and Food Safety, Istanbul Aydın University, Istanbul 34290 Turkey, email: b.sarici@hotmail.com*
[b]*Department of Food Engineering, Faculty of Engineering, Istanbul Aydın University, Istanbul 34290 Turkey, email: sukrukaratas@aydin.edu.tr*
[c]*Pamukova Vocational School, Sakarya University of Applied Sciences, Sakarya 54900 Turkey, email: altintig@subu.edu.tr*

Received 28 September 2021; Accepted 19 February 2022

ABSTRACT

The purpose of this investigation is to produce activated carbon from hazelnut shells by using chemical activation method of potassium carbonate. For the activation, the shells were milled and sieved in range of 50–150 mesh and then impregnation ratios were selected at the ranges of 1:1, 1:2 and 1:3. The carbonisation was carried out under the N_2 gas pressure with flow rate of 100 mL min^{-1} at 873.15 K for 120 min. The characterization of carbonization of activated carbon were executed with the X-ray diffraction, Fourier-transform infrared spectroscopy and scanning electron microscopy after drying samples and also in order to determine the adsorption capacity, the iodine and Methylene blue numbers were used. In this research, the microporous character of series of activated carbons has been analyzed using of the Brunauer–Emmett–Teller (BET) equation. N_2(BET) surface area was found to have the maximum BET area as 644 m^2 g^{-1}, the absorbants of iodine and Methylene blue numbers were determined 1,974 mg/I_2 and 489 mg g^{-1}, respectively for 70 mesh in the impregnation ratio of 1:2. In the addition to that the kinetic of Methylene blue adsorption were determined by the pseudo-second-order kinetic model and also the thermodynamic parameters were calculated to see whether the adsorption was spontaneous or not. The experimental data indicated that the adsorption isotherms were well matched by the Langmuir equilibrium isotherm equation given as 454.5 mg g^{-1} at 293 K.

Keywords: Activated carbon; Potassium carbonate; Hazelnut shell; Brunauer–Emmett–Teller; Iodine number; Kinetic; Adsorption; Methylene blue

1. Introduction

Activated carbon (AC) is obtained from a carefully controlled process of dehydration, carbonization and oxidation of organic substances. However, the most commonly used ones in commercial practice are peat, coal, lignite, wood and agricultural by-products such as coconut shell, almond shell, rice husks, etc. AC might be produced from almost all rich-in-carbon and cheap biomass with lower inorganic content [1]. Even though the main element belonging to activated carbon is carbon, its basic impurities are oxygen, hydrogen, nitrogen, and ash. Ash forms fundamentally from alkaline and alkaline earth metals [2]. The amount of such impurities and non-carbon materials the activated carbons have do vary in accordance with the major material used for activated carbon production, the period of activation and the conditions of carbonisation [3]. In recent years, scientific studies have increased significantly on low-cost raw material alternatives such as agricultural and industrial wastes to produce activated

* Corresponding author.

carbon [4]. hazelnut shells, containing approximately 50% of carbon, were transformed into activated carbon successfully and reported to be a good major material in order to produce high quality carbon [5]. Because hazelnut shell amount is equal to that of hazelnut kernel in weight, the residual hazelnut shells after obtaining the hazelnut kernels are of a significant matter of waste in the production region [6]. Production might be made by physical and chemical activation. Physical activation is a two-stage process. The material is carbonised in an inert atmosphere and then activated to produce porous structures by using steam or CO_2 as the activation agent [5]. Chemical activation, on the other hand, the raw material saturated by the activation agents such as KOH, K_2CO_3, $ZnCl_2$ and H_2SO_4 is heated in an inert atmosphere to achieve carbonisation and activation stage at the same time [7]. The advantages of chemical activation, when compared to physical activation, are lower energy and operational expenses, higher yield of carbon, wide surface area and more developed structure [6]. The yield of pyrolysis of the particle size in activated carbon and thus it's a bit of effect on the produced activated carbon is well-known. This effect is referred to slower heating mechanism (slower transmission speed) in the large particles and that results in reduced volatile oscillation [5]. AC has been used as an adsorbent in many applications for centuries due to its low cost and high adsorption capacity [8,9].

Applications of mesoporous activated carbons include drinking water purification, waste-water treatment, sweetener discolourization, food and chemical processing. On the other hand, microporous carbons are used for solvent recovery, gasoline emission control, cigarette filters and industrial emission gas treatment [5,8].

Textile dyes and organic wastewater of different industries are among the important reasons of environmental pollution [10]. Textile industry produces substantially wastewater containing colorants. Spreading of wastewater containing colorants is not only a source of concern owing to carcinogenic and toxicological effects on all living creatures but also a critical situation affecting the ecological balance adversely for aquatic creatures because that blocks the transmittance of the sunlight [11]. Methylene blue as a cationic dye is an important substance that should be considered because it is widely used in a number of sectors, its certain toxic effects on all living creatures and adsorbents are a model compound for measuring the dye adsorption capacity [12]. The basic problem of the contaminant effects of textile wastewater is the lack of a single treatment system to ensure the colour removal of wastewater due to its complex nature and rectify wastewater sufficiently [13]. To prevent the environmental pollution, organic contaminants should be removed from liquid wastes. Activated carbon is the most widely used adsorbent to remove organic contaminants led by liquid wastes [14–17].

There are different studies in the literature on the removal of dyestuffs. In their 2008 study, Yener et al. [18] examined the sorption rate and equilibrium parameters using granular and powdered activated carbon to remove Methylene blue. As a result, they found that the adsorption properties of powdered activated carbon are superior to granular activated carbon. Hosseini and Babaei [19] synthesized the graphene oxide (GO)/zinc oxide (ZnO) adsorbent in their research in 2017. Then they investigated the conditions for Methylene blue removal. The optimum pH was found at 4.5 for the dose of adsorbent as 2 g L^{-1} [19].

Turkey is in the lead for hazelnut production in the world by two out of three of the total crops. In this respect, hazelnut shell is an important raw material in Turkey to be turned into a value added product for both the region and the country as a renewable and cost-efficient raw material [2].

Carbonized ammonium chloride-impregnated and untreated almond shell and hazelnut shell samples in a flow of nitrogen at relatively low temperatures. It was observed that, chemical activation carried out at 350°C gave products with surface area values above 500 m^2 g^{-1}. However, the surface area values observed for the products obtained from untreated raw materials were about half of this value. It was also observed that, the surface area of products obtained from NH_4Cl-impregnated samples reached values of over 700 m^2 g^{-1} when the carbonization temperature was increased to 700°C [20]. Activated carbons from pistachio-nut shells, which are one type of lignocellulosic material, by a two-step physical method. They studied on the effects of the preparation variables on the activated carbon pore structure, followed by the optimization of these operating parameters. They found that the activation temperature and dwell time are the important parameters that affect the characteristics of the activated carbons obtained [21].

The objective of this study is to produce activated carbon from an agricultural waste by transforming grounded hazelnut shell into activated carbon with potassium carbonate and to investigate kinetic of adsorption, thermodynamic parameters and surface area of activated carbon by the Langmuir equilibrium and Brunauer–Emmett–Teller (BET) equation, also to characterize activated carbon with X-ray diffraction (XRD), Fourier-transform infrared spectroscopy (FTIR) and scanning electron microscopy (SEM) equipment's.

2. Material and method

2.1. Material

ACs were produced from hazelnut shells in this study. K_2CO_3 (potassium carbonate), NaOH (sodium hydroxide), sodium thiosulphate pentahydrate, potassium iodide and polysaccharide, HCl (hydrochloric acid) and MB (Methylene blue) with analytical grade were purchased from Merck, Germany supplied. The raw hazelnut shell was collected from Giresun, Turkey then dried and crushed in 2019. MB stock solution was prepared as 1,000 mg L^{-1}. The standard and working solutions were prepared by diluting stock solution with deionised water. The pH adjustments of the solutions were prepared with 0.1 M HCl and 0.1 M NaOH solutions and all chemicals were prepared daily.

2.2. Analytical measurements

During activated carbon production, Protherm brand PTF 12-105-900 model tube furnace was used. Wisestir brand MSH-20A model magnetic stirrer was used for heating and stirring procedures. Nüve brand FN500 model drying oven was used for all drying procedures. SEM images were

obtained using a Jeol brand JSM-6060LV model device to observe microscopic morphology changes of hazelnut shells, pre- and post-adsorption of activated carbons. The operating voltage was selected within in the range of (10–20 kV). The images were recorded via zoom between 1.000x and 300.000x, and in resolution between 50 × 10^3 – 200 nm. The FTIR analysis of adsorbent was carried out in the wavelength range of 400–4,000 cm^{-1} by using a PerkinElmer model spectrometer. The ultraviolet and visible light (UV-Vis) measurements were made by Shimadzu brand UV-2600 model spectrophotometer. Measuring range was at 665 nm and the pH values of solutions were recorded via the Mettler TOLEDO brand SevenCompact model device. The crystal structures of the samples were confirmed in an angle range of 10°–80° 2θ by a Rigaku brand X-ray diffractometer (XRD).

2.3. Preparation of activated carbons

Firstly, the raw material was washed thoroughly using distilled water to eliminate any adhering dirt sticking on the surface then it was dried at room temperature for 72 h after that the samples were dehydrated in an oven at 100°C overnight then they were ground into three different mesh sizes of 50, 70 and 150. The hazelnut shells with a net size of 50, 70 and 150 were encoded as HS1, HS2 and HS3, respectively, and kept in a desiccator for carbonization operations.

In this research, chemical activation of hazelnut shells was performed using 99% potassium carbonate (K_2CO_3). The imperation ratio of 1:1, 1:2 and 1:3 (HS:K_2CO_3). 10 g of K_2CO_3 were dissolved in 250 mL of distilled water then mixed with 10 g of hazelnut shells. The mixtures were kept in shaking incubator with 200 rpm at 313.15 K for 24 h to impregnate chemicals then the filtered samples were dried at 363.15 K for a day.

The carbonization of the impregnated samples were carried out in a 316 stainless steel tubular reactor with a length of 90 mm with an internal diameter of 105 mm (Protherm PTF 12) under nitrogen (N_2) gas flow (100 cm^3 min^{-1}), at a heating rate of 10°C/min then were held at 873.15 K for 2 h. It was then washed with distilled water to remove excess acid until the pH of the leached solution was around 4–5. The sample was then dried at 283.15 K min^{-1} for 24 h, crushed and sieved into an approximate uniform size of 1 mm. The production yield was calculated by the activated carbon that was gathered. The yield of the produced activated carbons was calculated by Eq. (1).

$$\text{Yield} = \frac{W_2}{W_1} \times 100\% \tag{1}$$

where W_1 = the weight of raw material (g), W_2 = the weight of activated carbon (g).

The notation and yields of produced activated carbons as per conditions are given in Table 1.

2.4. Yields of activated carbons activated by K_2CO_3

Table 1 given the % yield of nut shells for different mesh sizes. When these results were analyzed, it was observed that the yield soared as the ratio of K_2CO_3/raw material was increased and showed the same decrease in particle size as it did. Three activated carbons in the mesh range 50, 70 and 150 with the highest yield in Table 1 were chosen and coded as HSAC1 for 50 mesh 1:3 ratio, HSAC2 for 70 mesh 1:2 ratio and HSAC3 for 150 mesh 1:1 ratio. Yields for these three activated carbons (HSAC1, HSAC2, and HSAC3) were found to be 36.8%, 34.2%, and 31.2%, respectively. Those selected three activated carbons were used for characterisation and adsorption procedures.

2.5. Adsorption studies

MB solutions of different concentrations were prepared by diluting 1,000 mg L^{-1} stock MB solution. The adsorption processes were carried out in batch system, operational volume of 100 mL, Erlenmeyer's of 250 mL and shaking waterbath with stirring speed of 100 rpm. The effects of initial pH (2–9), adsorbent dosage (0.1–1 g L^{-1}), initial concentration (50–250 mg L^{-1}), contact time (5–180 min) and temperature (293, 303 and 313 K) to the adsorption of MB with activated carbon obtained from the shell of hazelnuts (HSACs) were analysed. Samples of 4 mL were taken at certain intervals and centrifuged at 3,000 rpm for 5 min during adsorption procedure, and after centrifugation the upper liquid was removed, and measurements were made using a UV-Vis spectrometer.

In the experiments, the % of colorant adsorbed was calculated by Eq. (2) as follows.

The percentage of MB dye adsorption was calculated using the following equation:

$$\text{Removal}(\%) = \frac{(C_o - C_e)}{C_o} \times 100 \tag{2}$$

where q_e refers to equilibrium dilution of MB (mg g^{-1}) absorbed over HSACs. C_o and C_e refer respectively to initial (mg L^{-1}) and equilibrium (mg L^{-1}) dilution of MB in the solution during equilibrium time.

3. Results and discussion

3.1. Chemical and morphological characterisation result

3.1.1. Results of proximate analysis on hazelnut shells

The proximate analysis [22–24] hazelnut shells of the highest yield in three different mesh ranges have been presented in Table 2. The quantity of fixed carbon was calculated by deducting that of moisture, ash, and volatile matter from 100.

Table 2 shows the results of proximate analysis of hazelnut shells in different mesh ranges. According to the literature, a biomass sample with a moisture content of less than 10% is recognized as the best raw material to produce activated carbon [25–28]. This ratio in our study is between 6.05 and 7.23. Upon evaluation of Table 3, we might report that the hazelnut shells used for our study are eligible for activated carbon production by their lower ash content (%), higher volatile matter content (%) and fixed carbon content (%). One of the key parameters to affect pyrolysis process is the volatile matter rate in the biomass. According to the literature, the volatile matter content in different biomass samples processed for

Table 1
Yields of activated carbons activated with K_2CO_3

Sample	Temperature (K)	Mesh spacing (Mesh)	K_2CO_3/raw material	Time (h)	Yield (%)
1	873.15	50	1:1	24	35.3
2	873.15	50	1:2	24	35.6
3	873.15	50	1:3	24	36.8
4	873.15	70	1:1	24	33.4
5	873.15	70	1:2	24	34.2
6	873.15	70	1:3	24	32.7
7	873.15	150	1:1	24	31.2
8	873.15	150	1:2	24	29.7
9	873.15	150	1:3	24	28.3

pyrolysis varies between 48% up to 87% [29] and that of hazelnut shells in three different mesh ranges in this study was confirmed to be between 64.91% up to 71.1%. Highly volatile matter in hazelnut shells is to be removed by the temperature during fixed carbon will remain as the component of activated carbon. One of the inorganic components in biomass structure is the ash content. According to the literature, it is well known that the ash content of different biomass samples varies between 0.1% up to 3.8% [30,31]. In this study, it was revealed that the ash content varied between 1.3% and 1.64%. When compared to the literature, hazelnut shells were considered to be a good starting material for hazelnut shell based activated carbon production due to their lower ash content [32].

Structural parameters of the produced activated carbons were evaluated, and the results are revealed in Table 3.

Table 3 shows the BET surface areas of the activated carbons we produce. The widest surface area, on the other hand, was reported as 644 m^2 g^{-1} in the impregnation ratio of 1:2 and carbonisation temperature of 873.15 K. Considering the surface area of commercial activated carbons to be between 300 and 2,000 m^2 g^{-1} [23], activated carbon produced from hazelnut shells gave the impression to be a good alternative in terms of the yield and the cost-effectiveness.

3.2. Results of characterisation

The FTIR spectrum of the before and after adsorption activated carbons (HSAC1, HSAC2 and HSAC3) of hazelnut shells (HS1, HS2 and HS3) in different mesh ranges is shown in Fig. 1a–c.

Fig. 1a–c show in (a) hazelnut shells before chemical activation, (b) activated carbon produced after chemical activation and carbonisation, and (c) FTIR spectrums of activated carbons after the adsorption of MB colorants of the hazelnut shells in the mesh range of 50–70–150. The large and broad distribution OH^- adsorption peaks at 3,400 cm^{-1} indicate the existence of alcohol, phenol, or carboxylic acids while asymmetric and symmetric C–H vibrations at 2,900 cm^{-1} indicate the existence aliphatic structures [3,18]. The peaks at approximately 1,750 cm^{-1} stem from olefinic C=C and C=O vibrations in the aromatic structures whereas the strong peaks at approximately 1,000 cm^{-1} stem from C–O vibrations. FTIR images of hazelnut shells have vivid and distinct peaks but the emphasis of OH^- peak of all mesh ranges of activated carbon decreased as in Fig. 1a–c. When FTIR spectrums of activated carbons are compared to that of raw materials, changes in the functional groups are confirmed. The O–H vibration band that can be seen between 3,400–3,300 cm^{-1} does not prevail among solid products. This is an expected result considering oxygen in the raw materials was removed by carbonisation and a carbon-based solid product remained after the aromatic structures were distorted [33,34].

Table 2
The proximate analysis of hazelnut shells

Proximate analysis (wt.%)	HS1	HS2	HS3
Moisture	6.05	6.51	7.23
Ash	1.64	1.53	1.30
Volatile matter	71.1	68.01	64.91
Fixed carbon[a]	21.21	23.95	26.56

[a]By difference

Qualitative and quantitative inspections of hazelnut shells in different mesh ranges and activated carbons produced from hazelnut shells were conducted by XRD spectrums to be acquired by X-ray diffraction spectroscopy. In Fig. 2a–c the results of XRD analysis on hazelnut shells in the mesh range of 50, 70 and 150 and produced activated carbons before and after the adsorption have been shown.

Fig. 2a–c show (a) hazelnut shells before chemical activation, (b) activated carbon produced after chemical activation and carbonisation, and (c) spectrums of activated carbons after the adsorption of MB of the hazelnut shells in the mesh range of 50-70-150 used for adsorption process. However, no peak is available in XRD spectrum because the produced activated carbons do not have a crystalline structure. Neither the activation procedures carried out nor the temperature changed the crystalline structure of raw material. Upon evaluation of the figures, broad distribution peaks are available, but the distinct peaks required for qualitative analyses cannot be seen. This is directly linked to the amorphous structure [35,36].

The SEM analysis was exercised in order to ascertain the surface morphology of the raw hazelnut shells in different mesh ranges (50, 70 and 150), activated carbons produced

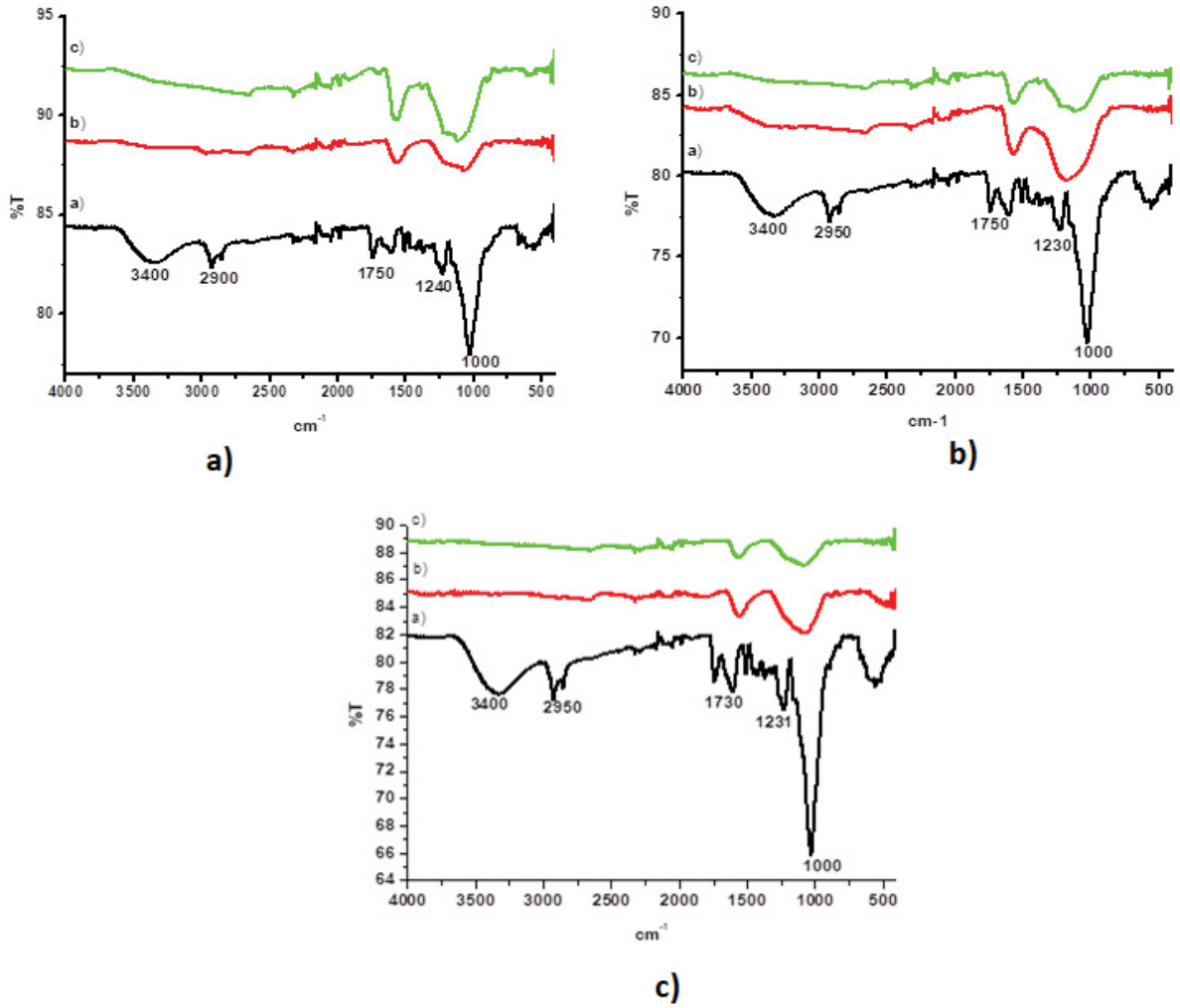

Fig. 1. FTIR of spectrums of (a) HSAC1, (b) HSAC2, and (c) HSAC3.

before adsorption from the hazelnut shells in those mesh ranges and activated carbons after adsorption. The respective SEM photos have been submitted between Figs. 3–5.

As raw hazelnut shells, the SEM photos of which have been given in Figs. 3–5, became activated; the pores were opened, and the typical honeycomb pattern of activated carbon was identified. When activated carbons in three different mesh ranges after adsorption were analysed and are given in Figs. 3–5, it was seen that the colorant had been absorbed by those combs and spread on the pores heterogeneously. When the SEM photo of raw material compared to that of activated carbon, the changes led by the chemical used and the heat treatment were clearly seen. It was confirmed as well that the activation process had formed pores by opening the closed channels [37–39].

3.3. Effect of pH on MB removal yield

The pH value is one of the most important factors that might affect the charge density of adsorbent and diluted ion concentration in the solution. For this reason, it has an indirect effect on the adsorption capacity [40]. The effect of pH on MB adsorption for activated carbon produced from three different mesh ranges was analysed in colorant concentration of 100 mg L^{-1} as 0.1 g/100 mL dose at 298 K. The dependency on the pH of the solution for the HSACs' MB removal yield has been shown in Fig. 6a and b.

The effect of pH on adsorption capacity is shown separately in Fig. 6a for three different HSACs. As pH increased, the adsorption of MB which is a cationic colorant, showed a significant increase as well. After the pH 6 was reached, the increase on adsorption intake was limited by active sites and adsorption, and the maximum value of pH 8 for three different HSACs was achieved. Adsorption capacity of HSACs in the mesh ranges of 50, 70 and 150 respectively was found as 99.17%, 99.23%, and 97.86%. The highest capacity was calculated for HSAC2 produced from hazelnut shells in the mesh range of 70.

3.4. Effect of mixing time on MB removal yield

The properties of the sorption centers and the retained material have a significant effect on the time required for the adsorption to reach equilibrium. There is

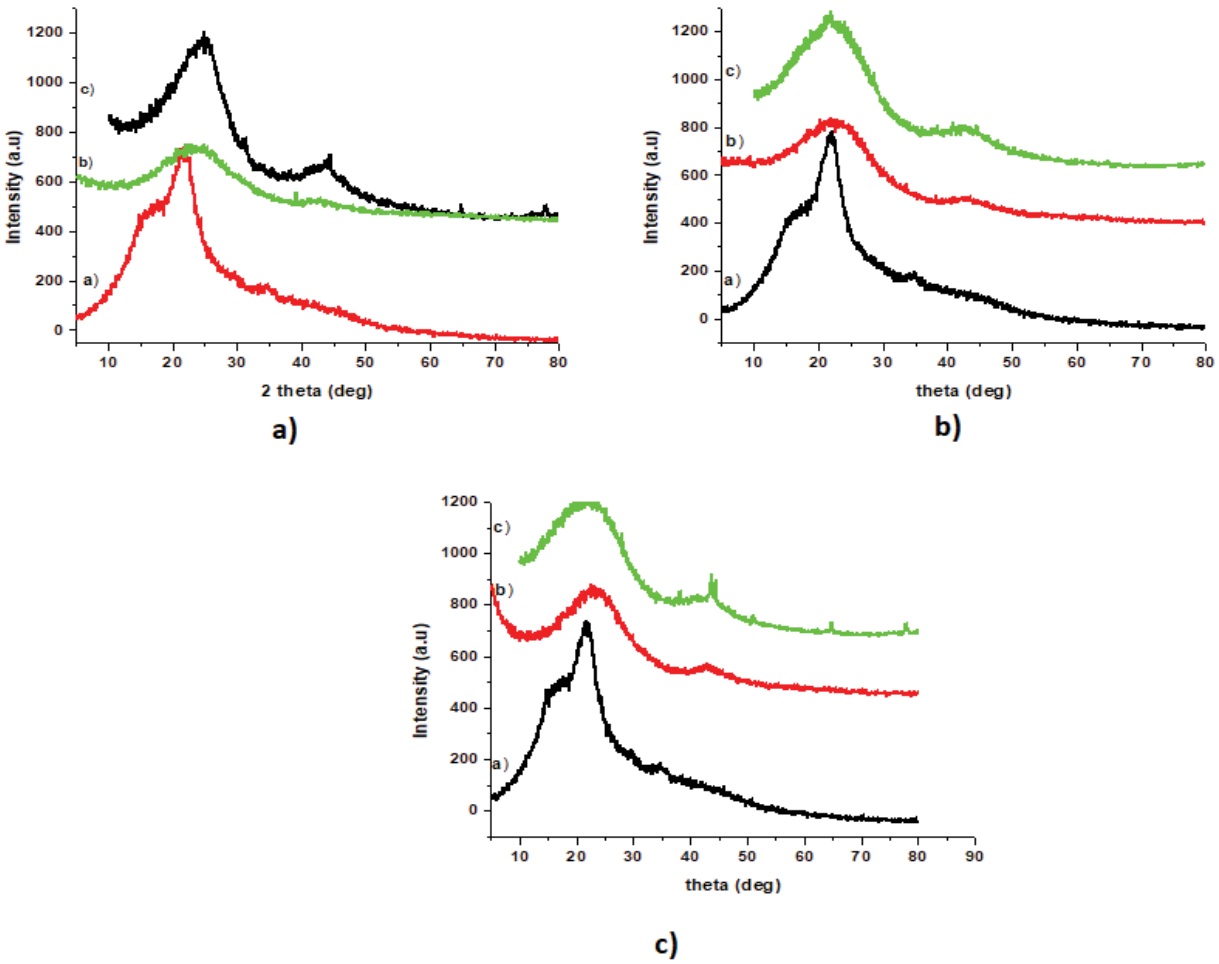

Fig. 2. Powder XRD patterns of (a) HSAC1, (b) HSAC2, and (c) HSAC3.

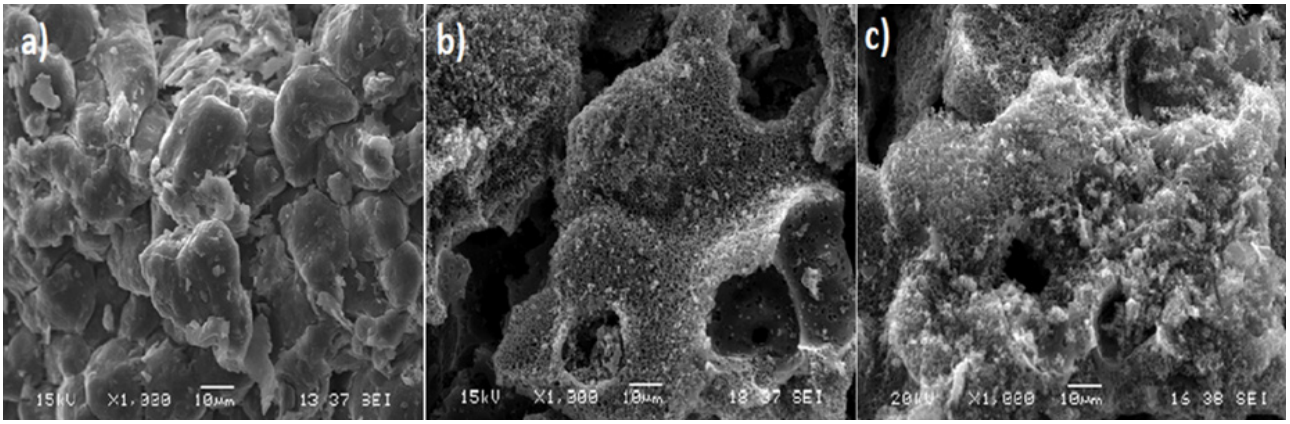

Fig. 3. SEM photographs of (a) HS1, (b) HSAC1 before adsorption, and (c) HSAC1 after adsorption.

a dispersion identified between diluted solid and liquid phases. Dispersion rate is the measurement of the equilibrium status in adsorption process [41]. The adsorption equilibrium time, the initial MB concentration in 100 mg L^{-1}, pH 8, 293 K and 0.1 g/100 mL adsorbent dose was processed in different mixing time for the HSACs in different mesh ranges and the results have been submitted in Fig. 6b as follows.

In Fig. 6b, the effect of adsorption equilibrium time on adsorption removal is observed for activated carbons in

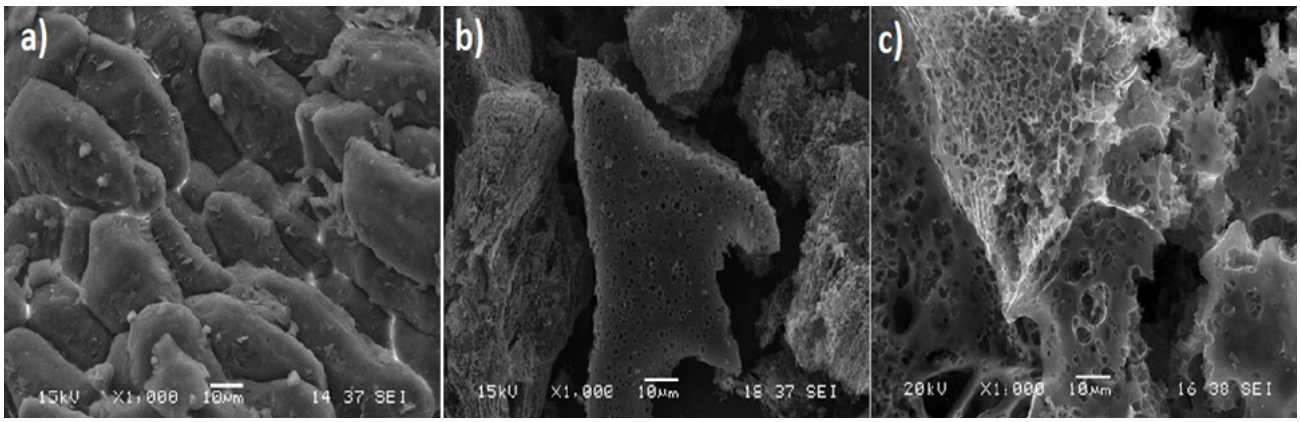

Fig. 4. SEM photographs of (a) HS2, (b) HSAC2 before adsorption, and (c) HSAC2 after adsorption.

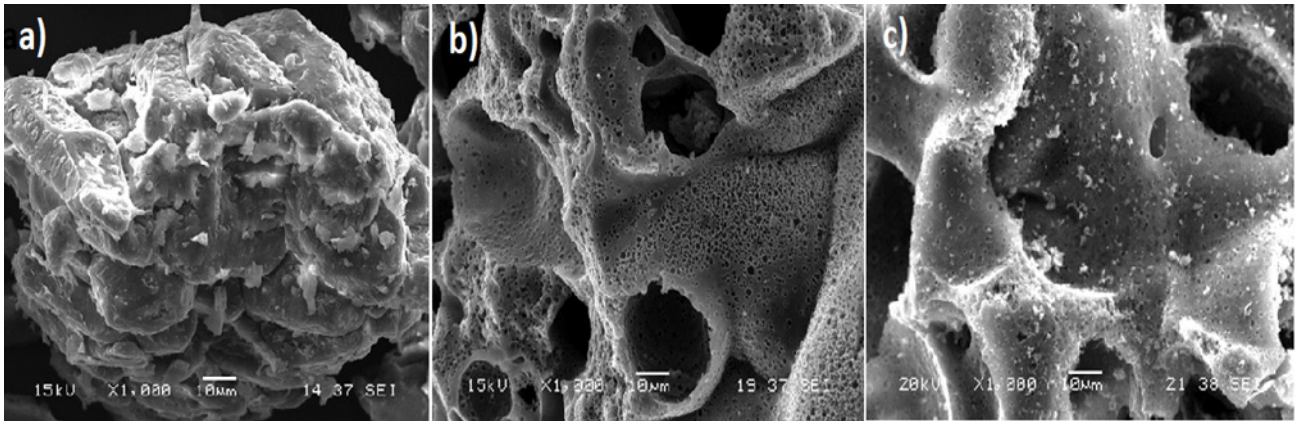

Fig. 5. SEM photographs of (a) HS3, (b) HSAC3 before adsorption, and (c) HSAC3 after adsorption.

three different mesh ranges. Adsorption equilibrium time for activated carbons in three different mesh ranges was observed to have increased much after 60 min despite the slight increase until 60 min, fixed at 90 min and reached the equilibrium optimally at 120 min by all the three samples. This is because the adsorbent reached the highest capacity to adsorb. Furthermore, the optimal stirring time for all analysed initial MB concentrations was decided to be 120 min. In the literature, Xue et al. [42] in their study on tobacco stalk to remove MB reported that 180 min was required for equilibrium contact time. This may be due to structure differences of raw materials.

3.5. Effect of adsorbent dose on MB removal yield

Adsorbent dose is one of the key factors that affects the removal yield. In the event that the adsorbent dose is insufficient, MB removal yield might decrease; on the contrary, flocculation might occur when adsorbent dose is redundant. The both affects the adsorption negatively [43–45]. In this study, the adsorbent dose was taken in five different values as 0.1, 0.2, 0.3, 0.4 and 0.5 g/100 mL at initial MB concentrations of 50, 70 and 150 mesh, pH 8 and 293 K. The effect of adsorbent dose on adsorption have been submitted in Fig. 6c as follows.

The highest yields by the samples in three different mesh ranges for MB removal was observed in the dose range of 0.1 g/100 mL. As might be seen in Fig. 8, the more the quantity increased the more the removal yield decreased. The highest yield among the three different mesh ranges was ascertained as 97.02% for the HSAC2 sample in the mesh range of 70. The lowest yield, on the other hand, was recorded as 86.02% in 0.5 g/100 mL for the HSAC3 sample in the mesh range of 150. In deference to those results, optimum adsorbent dose was taken as 0.1 g/100 mL for the collective experiments conducted afterwards.

3.6. Effect of initial MB concentration on MB removal yield

The effect of initial concentration on MB removal yield was investigated by activated carbons in three different mesh ranges in 293 K, pH 8 and 0.1 g L^{-1} adsorbent dose. The results for five different initial MB concentrations (50, 100, 150, 200 and 250 mg L^{-1}) have been submitted in Fig. 6d as follows.

The effect of the initial MB concentration on adsorption was investigated in the concentration range of 50 to 250 mg g^{-1} using 0.1 g of HSACs at the solution pH value (8) at a temperature of 293 K. When the initial concentration of MB was increased from 50 to 250 mg g^{-1}, the percentage of

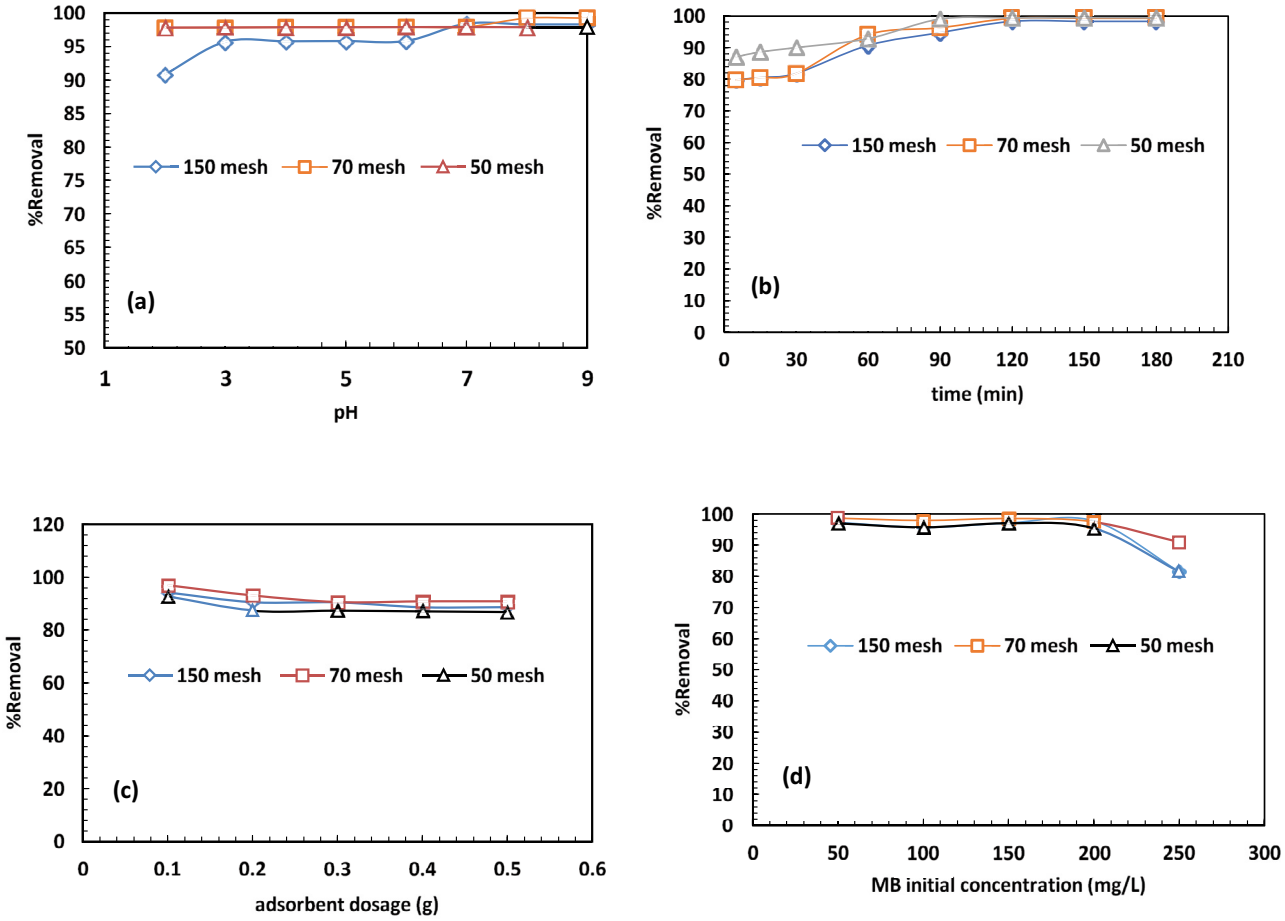

Fig. 6. (a) Effect of MB removal yield on the pH of solution (initial MB concentration: 100 mg L^{-1}, temperature: 298 K, adsorbent dose: 0.1 g/100 mL). (b) Mixing time effect the removal yield of MB (initial concentration: 100 mg L^{-1}, temperature: 298 K and pH: 8, adsorbent dose: 0.1 g/100 mL). (c) Adsorbent dose effect on the removal yield of MB (temperature: 293 K and pH: 8). (d) The initial MB concentration effect on the removal yield of MB (temperature: 293 K, pH: 8, adsorbent dose: 0.1 g/100 mL).

MB removal decreased from 98.65% to 81.33%. It is clearly seen in Fig. 6d that the adsorption yield for the HSACs in the different mesh ranges analysed decreased by the increase of initial MB concentration.

3.7. Effect of temperature on the amount of removed MB

The effect of temperature on MB removal yield was investigated for pH 8 at three different temperatures as 293, 303 and 313 K in 0.1 g/100 mL dose and 100 mg L^{-1} initial colorant concentration. The change of MB adsorption by temperature has been submitted in Fig. 7 as follows.

As in Fig. 7a, the amount of removed MB increased linearly by the rising temperature. This result is reckoned to have emanated from the increasing mobility of MB molecules from the solution to the surface by rising temperature [46].

3.8. Adsorption thermodynamics

Temperature is one of the most important parameters that affects the interaction and kinetics between the adsorption agent and the colorant. Adsorption is analysed thermodynamically by ascertaining enthalpy change, entropy change, free enthalpy change and equilibrium constant [47]. In order to evaluate the effect of temperature on the adsorption between HSACs and MB, adsorption enthalpy ($\Delta H°$), entropy ($\Delta S°$) and Gibbs free energy ($\Delta G°$) were calculated by thermodynamic parameters Eqs. (4)–(7) [48]. $\Delta G°$ parameter was calculated by taking instant dispersion constant (K_D) into consideration.

$$\Delta G° = -RT \ln K_D \tag{3}$$

$$\ln K_D = \frac{b_2}{b_1} \tag{4}$$

$$\Delta G° = \Delta H° - T\Delta S° = -RT \ln K_D \tag{5}$$

$$\ln K_D = -\frac{\Delta H°}{RT} + \frac{\Delta S}{R} \tag{6}$$

Enthalpy change ($\Delta H°$) and entropy change ($\Delta S°$) were determined by the slope-intercept formula $\ln K_D$ against $1/T$ chart. The value b_2 refers to the adsorption capacity in the equilibrium time (mg g^{-1}) and b_1 refers to colorant concentration remaining in the liquid phase in the

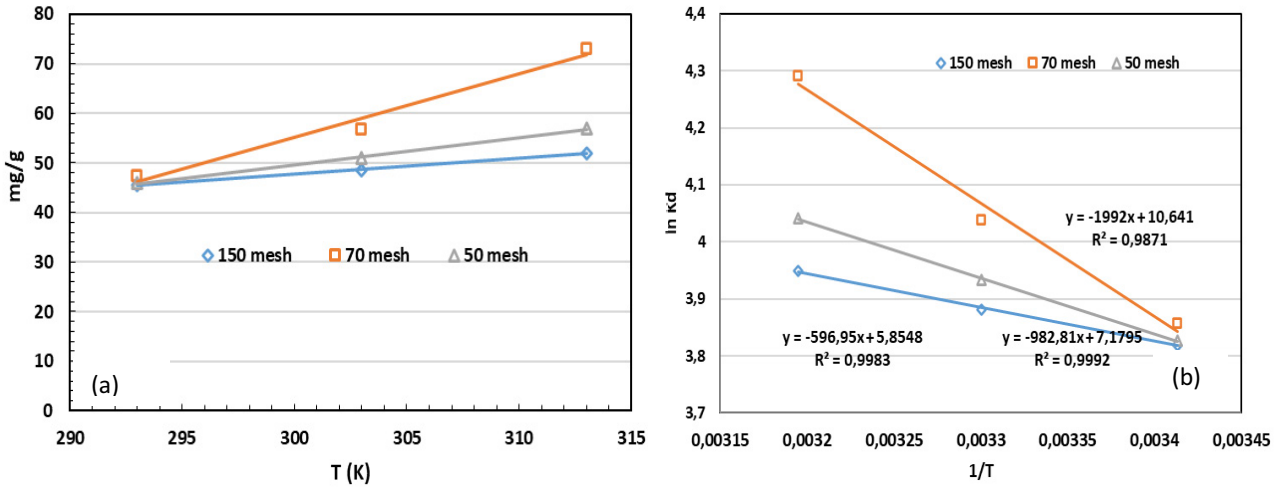

Fig. 7. (a) Temperature effect on the amount of removed MB and (b) variation of $\ln K_D$ with $1/T$.

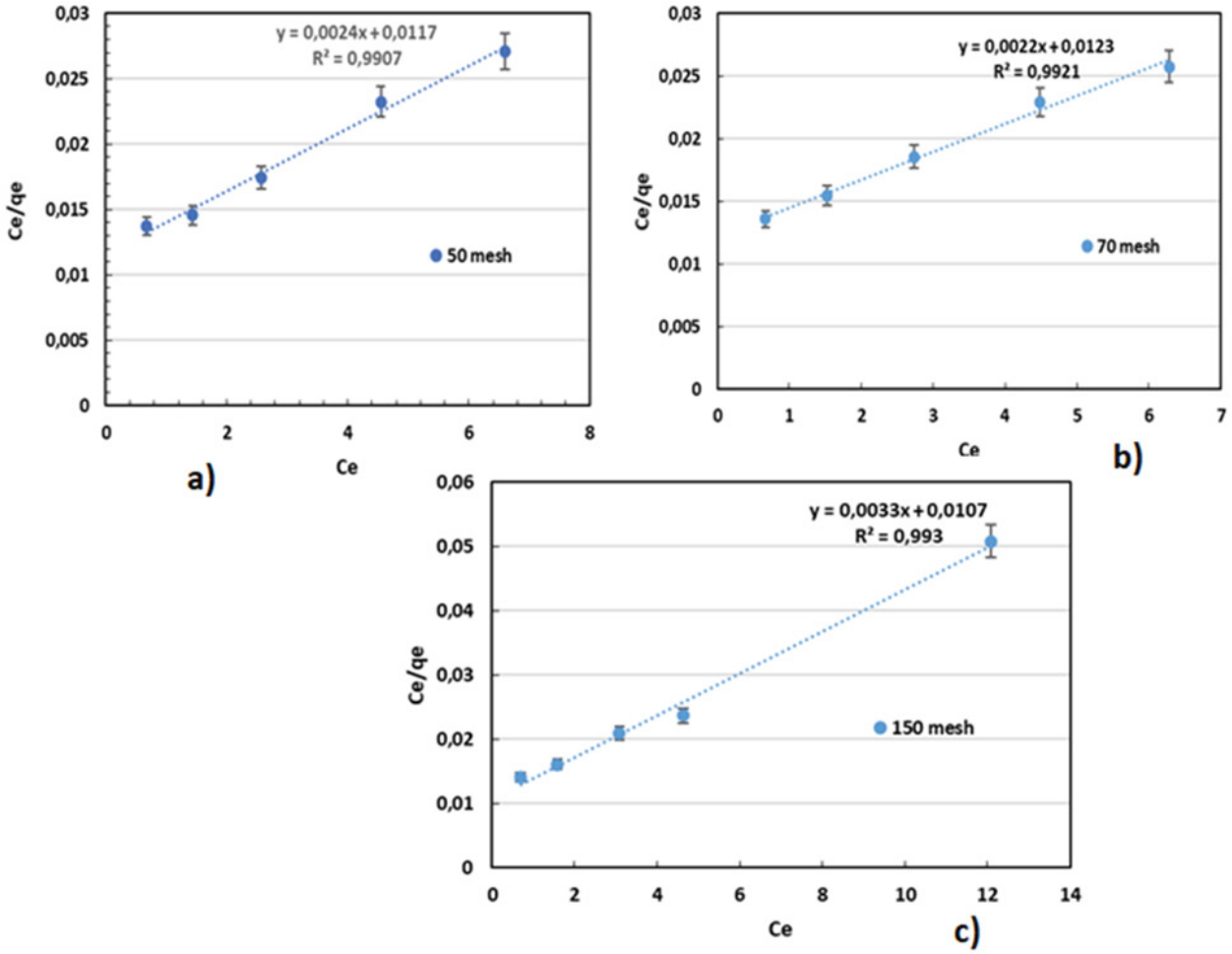

Fig. 8. Langmuir isotherm plots obtained for the adsorption MB onto (a) HSAC1, (b) HSAC2, and (c) HSAC3.

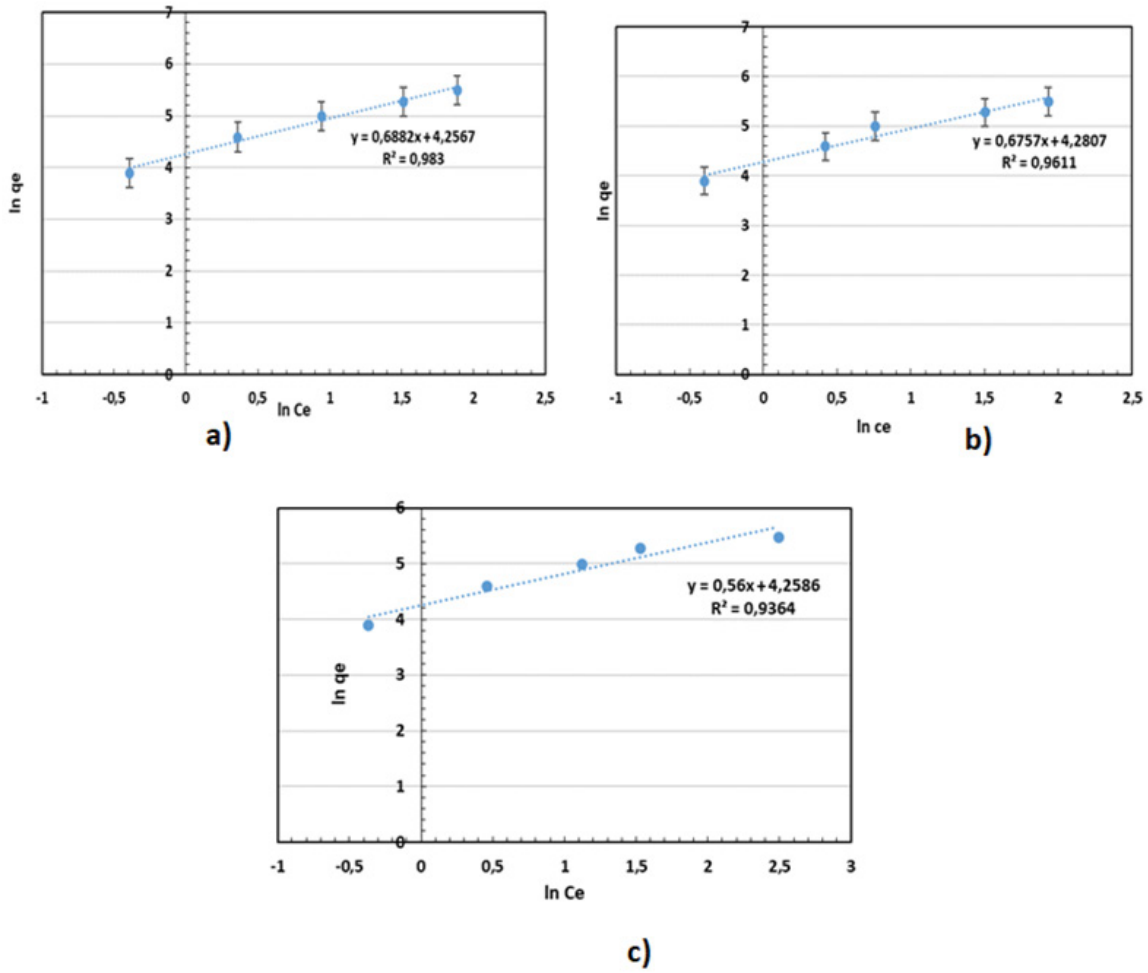

Fig. 9. Freundlich isotherm plots obtained for the adsorption MB onto (a) HSAC1, (b) HSAC2, and (c) HSAC3.

equilibrium time (mg L^{-1}). T and R are temperature (K) and gas consonant (8.314 J mol^{-1} K^{-1}) respectively [49].

The thermodynamic parameters of the MB adsorption onto activated carbons (HSAC1, HSAC2 and HSAC3) have been submitted in Table 4 as follows.

As might be seen in Table 4, $\Delta G°$ value in the three samples (HSAC1, HSAC2 and HSAC3) was calculated as –9.62, –10.51 and –10.81 kJ mol^{-1} respectively. In addition, Gibbs free energy –20 and 0 kJ mol^{-1} to be in the range of adsorption physical, –80 and –400 kJ mol^{-1} in the range of adsorption is chemical [48]. Obtaining the $\Delta G°$ value in negative points indicated that the MB adsorption onto HSACs occurred spontaneously. The decrease in the $\Delta G°$ value by the rising temperature propounds that higher temperature will ease the adsorption [50]. Therefore, it was revealed by $\Delta G°$ that the MB adsorption at 313 K is more practicable than it is at 293 and 303 K. $\Delta H°$ value in three samples was found as 7.56, 16.87 and 5.07 kJ mol^{-1} respectively. Obtaining $\Delta H°$ value in positive points suggested that the process is endothermic due to rising temperature. Rising temperature leads diffusion velocity of adsorbent molecules. Consequently, the particles in the external boundary layer and internal pores of the adsorbent reduces the viscosity of aqueous solution. The Langmuir and Freundlich isotherm graphs are shown in

Table 3
Surface characteristics of activated carbons

Sample	BET surface area (m^2 g^{-1})	Iodine number (mg/I_2)	Methylene blue number (mg g^{-1})	Total pore volume (cm^3 g^{-1})	*t*-plot micropore volume (cm^3 g^{-1})	Mesopore volume (cm^3 g^{-1})
HSAC1	344.00	1,974.00	476.00	0.052	0.28	n.d.
HSAC2	644.00	1,871.00	489.00	0.232	0.29	n.d.
HSAC3	472.00	1,632.00	473.00	0.120	0.35	n.d.

Figs. 8 and 9. Obtaining ΔS value in positive, on the other hand, refers to escalating disorder in solid-solution and the increase in randomness in the solid–liquid interface during adsorption [49].

3.9. Adsorption isotherms

Adsorption bears a resemblance to an equilibrium reaction. When solution is brought into contact with an adsorption agent in a certain amount, the dilution of the substance adsorbed in the solution decreased until the adsorption agent is balanced with those on its surface. After the adsorption equilibrium is ensured, the dilution of the substance adsorbed in the solution phase remains constant [51]. The amount adsorbed by an adsorbent agent is the function of the dilution and temperature of the substance adsorbed. In general, the quantity of substance adsorbed is confirmed as a function of dilution at constant temperature. The conclusion function called adsorption isotherm is achieved by recording in the chart the adsorbed dissolved amount in unit adsorption agent gravity against dissolved concentration remaining in the solution balanced at constant temperature. Langmuir and Freundlich adsorption isotherms were used in order to ascertain the isotherm models with the HSACs adsorption agents and the maximum adsorption capacity of MB adsorption [51,52].

Langmuir isotherm model assumes the adsorption to have occurred on a homogenous surface and as single layer. Moreover, Langmuir acknowledges that all active sites have equal energy and affinity against the molecules to be adsorbed [51]. The linear formulation of this model has been submitted in Eq. (8) as follows.

$$\frac{C_e}{q_e} = \frac{1}{q_m K_L} + \frac{1}{q_m} C_e \tag{7}$$

where C_e is the adsorbate concentration in the solution following the adsorption (mg L^{-1}), q_e is adsorbed amount onto adsorbent (mg g^{-1}), K_L is isotherm coefficient (L mg^{-1}), q_{max} is maximum adsorption capacity of adsorbent (mg g^{-1}).

The equilibrium data were calculated, if q is max, as 416.66, 434.78 and 303.03 mg g^{-1} by the correlation coefficient (R^2) for HSAC1, HSAC2 and HSAC3 as 0.99, 0.99 and 0.98 respectively.

Freundlich isotherm model assumes the multi-layer coating of adsorbent surface by adsorbent molecules [53]. This linear formulation has been submitted in Eq. (8) as follows.

$$\ln q_e = \ln K_f + \frac{1}{n} C_e \tag{8}$$

where q_e refers to equilibrium concentration (mg g^{-1}) of adsorbate onto surface of adsorbent, C_e refers to adsorbate (mg L^{-1}) in solution, K_f and n refer to Freundlich's constants.

Langmuir and Freundlich isotherm constant acquired by calculations have been submitted in Table 5.

When Table 5 in which Langmuir and Freundlich isotherm constants are provided together is assessed, it might be confirmed that the correlation coefficient (R^2) of Langmuir isotherm was around the range of 0.99 the correlation coefficient (R^2) of Freundlich isotherm was between the range of 0.94–0.98 in three different mesh ranges. The highest maximum adsorption capacity was 454.54 mg g^{-1} for HSAC2 sample while the highest maximum adsorption capacity was 303.03 mg g^{-1} for HSAC3 sample. Based upon those results, it might be reported that the Langmuir model for MB adsorption onto activated carbon is more compatible. Furthermore, it might be confirmed that the adsorption occurred as single layer in three different mesh ranges due to the compatibility to Langmuir model.

3.10. Kinetic studies

In order to identify the adsorption kinetics, the data obtained from experimental study were analysed by pseudo-first-order and pseudo-second-order. Kinetic studies were carried out with HSACs produced from hazelnut shells in the mesh range of 50, 70 and 150 in initial MB concentration of 100 mg L^{-1} at 293 K by 0.1 g L^{-1} adsorbent dose. The kinetic model by pseudo-first-order has been defined in Eq. (10) as follows [54].

$$\log\left(q_e - q_t\right) = \log\left(q_e\right) - \frac{k_1}{2.303} t \tag{9}$$

where q_e (mg g^{-1}) and q_t (mg g^{-1}) refer to the absorbed quantity of the adsorbate in equilibrium time and at any t time and k_1 (min^{-1}) refers to the rate constant. The k_1 and q_e values

Table 4
Thermodynamic parameters calculated for MB adsorption onto HSACs

Sample	T (K)	$\Delta G°$ (kJ mol^{-1})	$\Delta S°$ (kJ mol^{-1} K^{-1})	$\Delta H°$ (kJ mol^{-1})
	293	–9.62		
HSAC1	303	–10.51	59.00	7.56
	313	–10.81		
	293	–9.39		
HSAC2	303	–10.17	88.40	16.87
	313	–11.166		
	293	–9.30		
HSAC3	303	–9.78	49.5	5.07
	313	–10.28		

are calculated by the slope-intercept form of the $\ln(q_e - q_t)$ and t chart.

The kinetic data obtained by pseudo-first-order for HSACs in three different mesh ranges with the initial concentration of 100 mg L^{-1} are shown in Fig. 10a and Table 6. The R^2 value between those variables were found between the range of 0.90–0.95.

The kinetics mechanism of MB adsorption onto HSACs samples was investigated by the pseudo-second-order model formula [55].

$$\frac{t}{q_t} = \left[\frac{1}{k_2 q_e^2}\right] + \frac{1}{q_e} t \tag{10}$$

where k_2 (g mg^{-1} min^{-1}) refers to the constant of second-order rate constant. The q_e and k_2 values are determined based on the plot of t/q_t vs. t.

The kinetic results obtained from HSACs produced from different mesh ranges have been submitted in Table 6.

Pseudo-first-order and pseudo-second-order results of activated carbons produced from hazelnuts in three different mesh ranges are given in Table 6. The adsorption capacity ($q_{e,\exp}$) value propounded experimentally in Table 6 under ideal conditions should be close to the calculated adsorption capacity ($q_{e,\text{cal}}$) value. In Table 6, the adsorption process does not comply with the velocity requirements of pseudo-first-order due to the difference between $q_{e,\exp}$ and $q_{e,\text{cal}}$, and correlation coefficient value's not being close to 1 [56]. On the other hand, very high correlation coefficient was achieved by pseudo-second-order kinetic model. Besides, the q_e values obtained from the experimental data and calculated theoretically are very close to each other. Based upon those results, the colorant adsorption by the activated carbons produced from hazelnut shells with K_2CO_3 might be reported to be pseudo-second-order. There are similar results in the literature were given in [56,57].

3.11. Comparison of the developed adsorbent in terms of adsorption capacity

Adsorption capacity is one of the key parameters in colorant removal. In the Table 7, the $q_{\max}$ values for MB removal by using HSACs adsorbents were compared to adsorbents in different types subject to chemical activation with K_2CO_3 in the literature [56–61].

Upon evaluation of adsorption capacities of the activated carbon samples produced by K_2CO_3 chemical activation given in Table 8, it was confirmed that the adsorption capacities of the produced HSAC1, HSAC2 and HSAC3 samples had been higher than those of the other samples. The highest adsorption capacity in this study was ascertained to be 454.54 mg g^{-1} for the HSAC2 sample.

3.12. Desorption and recovering

To evaluate whether samples (HSAC1, HSAC2 and HSAC3) can be recycled for adsorption of MB, the samples used for the adsorption with MB were recovered simply by filtering with filter paper, washed with ethanol and distilled water several times, dried at 60°C and used again for six times without any obvious activity loss (Fig. 11).

Table 5
Langmuir and Freundlich isotherm constants obtained for 50, 70 and 150 mesh

Sample (mesh)	Langmuir isotherm			Freundlich isotherm		
	q_m (mg g^{-1})	K_L (L mg^{-1})	R^2	K_f	n (L mg^{-1})	R^2
HSAC1	416.66	0.20	0.99	70.58	1.45	0.98
HSAC2	454.54	0.18	0.99	72.29	1.48	0.96
HSAC3	303.03	0.30	0.99	70.68	1.78	0.94

Table 6
Comparison of MB adsorption capacities of HSACs produced by K_2CO_3 activation with different adsorbent types reported in the literature

Adsorbent	pH	Temperature (K)	Dosage (g mL^{-1})	C_0 (mg L^{-1})	Adsorption capacity (mg g^{-1})	References
Peels of fruits	9.0–10.0	298	0.6/100	100–500	59.9	[56]
Macadamia nuts shells	–	298	0.5/100	70	261.52	[57]
Pistachio nut shells	–	298	0.025/100	20–220	277.8	[58]
Cocos nucifera L.	8.0	298	0.1/100	250	15.775	[59]
Defatted olive cake	7.0	303	0.2/200	25–400	–	[60]
Clinoptilolite	7.0	293	0.28–2.25	13	43.2	[61]
HSAC1	8.0	293	0.1/100	50–250	416.66	This study
HSAC2	8.0	293	0.1/100	50–250	454.54	This study
HSAC3	8.0	293	0.1/100	50–250	303.03	This study

Table 7
Kinetic results determined based on pseudo-first-order and pseudo-second-order kinetic models

	Pseudo-first-order				Pseudo-second-order		
mesh	$q_{e,exp}$	k_1, min^{-1}	$q_{e,cal}$ (mg g^{-1})	R^2	k_2 (g mg^{-1} min^{-1})	$q_{e,cal}$ (mg g^{-1})	R^2
50	97.095	0.023	24.065	0.95	0.24	102.04	0.99
70	99.295	0.024	26.493	0.95	0.25	99.00	0.99
150	97.50	0.063	44.106	0.90	0.29	100.00	0.99

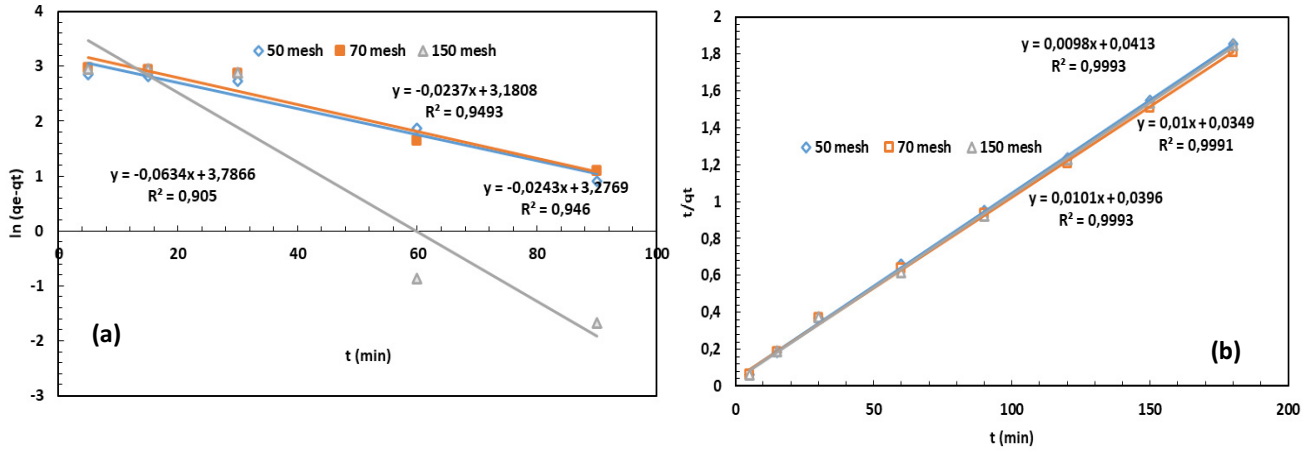

Fig. 10. (a) Pseudo-first-order kinetic modeling results obtained for MB adsorption onto 50, 70 vs. 150 mesh HSACs and (b) pseudo-second-order kinetic results obtained for MB adsorption onto HSACs (initial MB concentration: 100 mg L^{-1}, adsorbent dose: 0.1 g/100 mL, pH: 8, temperature: 298 K).

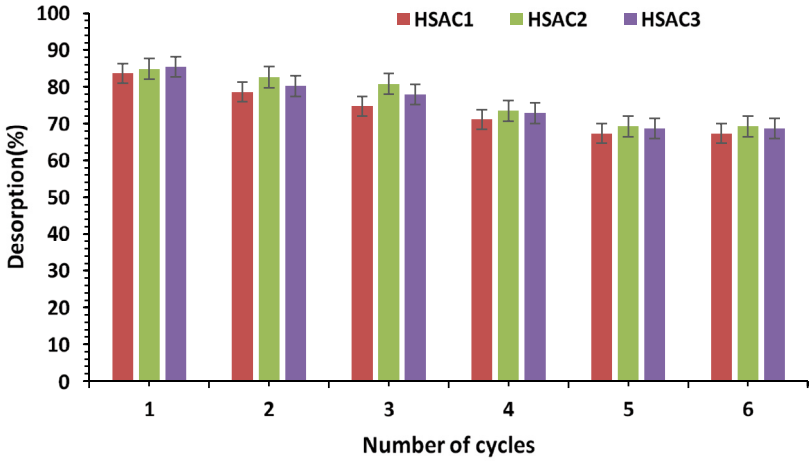

Fig. 11. The adsorption efficiency of for MB adsorption remained stable throughout six consecutive cycles of reuse.

The amount of MB adsorbed onto the HSACs sorbent resulted in a reduction of approximately 18.15% during desorption between 1–6 cycles. Recycling rates dropped from 85.47% to 67.32% gradually, whereas no decrease was observed during the adsorption cycles. However, in the first and six desorption cycles, a decrease of 18.15% was seen. These results show that the HSACs sorbent is important for reusability.

4. Conclusion

This study is mainly aimed at the use of activated carbons produced from hazelnut shells in different mesh ranges (HSACs) as adsorbents. It is of vital importance for local industry and ecology to use activated carbons produced from hazelnut shells as adsorbent instead of high-cost commercial products. In the second-stage of the study, the effectiveness

of HSACs adsorbents characterized in the removal of MB from aqueous solutions was experimentally carried out by equilibrium, kinetic, thermodynamic and recovery studies. Adsorption isotherm studies were shown that the equilibrium data are consistent with the Langmuir isotherm model and that the optimum temperature for all HSACs adsorbents in MB adsorption is 313 K, the contact time is 60 min and the initial pH value is 8. The highest maximum adsorption capacity of HSACs adsorbents was found to be 454.54 mg g^{-1} in the HSAC2 sample. Thermodynamic calculations have shown that the adsorption process has spontaneous and endothermic characteristics. Kinetic studies have revealed that the pseudo-second-order model is more compatible to identify the adsorption mechanism for HSACs in three different mesh ranges. The recovery work was repeated 6 times using a shaker. Recycling rates dropped from 85.47% to 67.32% gradually, whereas no decrease was observed during the adsorption cycles. However, in the first and six desorption cycles, a decrease of 18.15% was seen. It is recommended to use activated carbons produced from hazelnut shells in different mesh ranges (HSACs) for MB removal from aqueous solutions due to its cost-effective and easy-to-use advantages.

References

[1] O.J. Oginni, Characteristics of Activated Carbons Produced from Herbaceous Biomass Feedstock, Graduate Theses, Dissertations, and Problem Reports, Department of Wood Science and Technology, ProQuest LLC, Virginia, 2018. Available at: https://researchrepository.wvu.edu/etd/3719

[2] S.N. Andrade, C.M. Veloso, R.C.I. Fontan, R.C.F. Bonomo, L.S. Santos, M.J.P. Brito, G.A. Diniz, Chemical-activated carbon from coconut (*Cocos nucifera*) endocarp waste and its application in the adsorption of β-lactoglobulin protein, Rev. Mex. Ing. Quim, 17 (2018) 463–475.

[3] J. Changle, Lignocellulosic Biomass Derived Activated Carbon for Energy Storage and Adsorption, Graduate Theses, Dissertations, and Problem Reports, ProQuest LLC, 2019. Available at: https://researchrepository.wvu.edu/etd/7446

[4] D. Angin, A. Ilci, Removal of 2,4-dichlorophenoxy acetic acid from aqueous solutions by using activated carbon derived from olive-waste cake, Desal. Water Treat., 82 (2017) 282–291.

[5] E. Zafer Hoşgün, B. Bozan, Effect of different types of thermochemical pretreatment on the enzymatic hydrolysis and the composition of hazelnut shells, Waste Biomass Valorization, 7 (2020) 3739–3748.

[6] S. Sharifan, A Comparative Optimisation Study of Activated Carbon Production from Hazelnut Shells by Thermal and Microwave Heating Methods, Imperial College London, 2013, pp. 1–349.

[7] Y. Baran, H.S. Gökçe, M. Durmaz, Physical and mechanical properties of cement containing regional hazelnut shell ash wastes, J. Cleaner Prod., 259 (2020) 120965, doi: 10.1016/j.jclepro.2020.120965.

[8] H.M.H. Gad, A.A. El-Sayed, Activated carbon from agricultural by-products for the removal of Rhodamine-B from aqueous solution, J. Hazard. Mater., 168 (2009) 1070–1081.

[9] T. Kopac, Hydrogen storage characteristics of bio-based porous carbons of different origin: a comparative review, Int. J. Energy Res., 45 (2021) 20497–20523, doi: 10.1002/er.7130.

[10] S. Abbasi, M. Hasanpour, The effect of pH on the photocatalytic degradation of methyl orange using decorated ZnO nanoparticles with SnO_2 nanoparticles, J. Mater. Sci. - Mater. Electron., 28 (2017) 1307–1314.

[11] N. Yılmaz, O. Alagöz, Adsorption of Methylene blue on activated carbon prepared by chemical activation method from the pomegranate husks, El-Cezerî J. Sci. Eng., 6 (2019) 817–829.

[12] E. Menya, P.W. Olupot, H. Storz, M. Lubwama, Y. Kiros, Production and performance of activated carbon from rice husks for removal of natural organic matter from water: a review, Chem. Eng. Res. Des., 129 (2018) 271–296.

[13] E. Altıntıg, I. Acar, H. Altundag, O. Ozyıldırım, Production of activation carbon from rice husk to support Zn^{2+} ions, Fresenius Environ. Bull., 24 (2015) 1–8.

[14] Y. Kuang, X. Zhang, S. Zhou, Adsorption of Methylene blue in water onto activated carbon by surfactant modification, Water, 12 (2020) 587, doi: 10.3390/w12020587.

[15] K. Grace Pavithra, P. Senthil Kumar, V. Jaikumar, P. Sundar Rajan, Removal of colorants from wastewater: a review on sources and treatment strategies, J. Ind. Eng. Chem., 75 (2019) 1–19.

[16] S. Yadav, A. Asthana, R. Chakraborty, B. Jain, A.K. Singh, S.A.C. Carabineiro, Md. A.B.H. Susan, Cationic dye removal using novel magnetic/activated charcoal/β-cyclodextrin/alginate polymer nanocomposite, Nanomaterials (Basel), 10 (2020) 170, doi: 10.3390/nano10010170.

[17] U. Tyagi, Adsorption of dyes using activated carbon derived from pyrolysis of vetiveria zizanioides in a fixed bed reactor, Groundwater Sustainable Dev., 10 (2020) 100303, doi: 10.1016/j.gsd.2019.100303.

[18] J. Yener, T. Kopac, G. Dogu, T. Dogu, Dynamic analysis of sorption of Methylene blue dye on granular and powdered activated carbon, Chem. Eng. J., 144 (2008) 400–406.

[19] S.A. Hosseini, S. Babaei, Graphene oxide/zinc oxide (GO/ZnO) nanocomposite as a superior photocatalyst for degradation of Methylene blue (MB)-process modeling by response surface methodology (RSM), J. Braz. Chem. Soc., 28 (2017) 299–307.

[20] S. Balcı, T. Doğu, H. Yücel, Characterization of activated carbon produced from almond shell and hazelnut shell, J. Chem. Tech. Biotechnol., 60 (1994) 419–426.

[21] T. Yang, A.C. Lua, Characteristics of activated carbons prepared from pistachio-nut shells by physical activation, J. Colloid Interface Sci., 267 (2003) 408–417.

[22] ASTM D4442-20, Standard Test Methods for Direct Moisture Content Measurement of Wood and Wood-Based Materials, West Conshohocken, ASTM International, PA, 2020.

[23] ASTM E1755-01, Standard Test Method for Ash in Biomass, West Conshohocken, ASTM International, PA, 2020.

[24] ASTM E872-82, Standard Test Method for Volatile Matter in the Analysis of Particulate Wood Fuels, West Conshohocken, ASTM International, PA, 2019.

[25] T.E. Oladimeji, B.O. Odunoye, F.B. Elehinafe, O.R. Obanla, O.A. Odunlami, Production of activated carbon from sawdust and its efficiency in the treatment of sewage water, Heliyon, 15 (2021) e05960, doi: 10.1016/j.heliyon.2021.e05960.

[26] I. Ozdemir, M. Şahin, R. Orhan, M. Erdem, Preparation and characterization of activated carbon from grape stalk by zinc chloride activation, Fuel Process. Technol., 125 (2014) 200–206.

[27] V. Balasundram, N. Ibrahim, R. Md. Kasmani, Mohd. Kamaruddin Abd. Hamid, R. Isha, H. Hasbullah, R.R. Ali, Thermogravimetric catalytic pyrolysis and kinetic studies of coconut copra and rice husk for possible maximum production of pyrolysis oil, J. Cleaner Prod., 167 (2017) 218–228.

[28] M.S. Ahmad, M.A. Mehmood, O.S. Al Ayed, G. Ye, H. Luo, M. Ibrahim, U. Rashid, I.A. Nehdi, G. Qadir, Kinetic analyses and pyrolytic behavior of Para grass (*Urochloa mutica*) for its bioenergy potential, Bioresour. Technol., 224 (2017) 708–713.

[29] R. Saidur, E.A. Abdelaziz, A. Demirbas, M.S. Hossain, S. Mekhilef, A review on biomass as a fuel for boilers, Renewable Sustainable Energy Rev., 15 (2011) 2262–2289.

[30] O. Bag, K. Tekin, Production and characterization of hydrothermal carbon from waste lignocellulosic biomass, J. Fac. Eng. Archit. Gazi Univ., 35 (2020) 1063–1076.

[31] N. Söyler, J.L. Goldfarb, S. Ceylan, M.T. Saçan, Renewable fuels from pyrolysis of *Dunaliella tertiolecta*: an alternative approach to biochemical conversions of microalgae, Energy, 120 (2017) 907–914.

[32] X. Jian, X. Zhuang, B. Li, X. Xu, Z. Wei, Y. Song, E. Jiang, Comparison of characterization and adsorption of biochars

produced from hydrothermal carbonization and pyrolysis, Environ. Technol. Innovation, 10 (2018) 27–35.
[33] E. Pehlivan, Utilization of activated carbon produced from fruit juice industry solid waste for the adsorption of reactive red (procion red MX-5B) from aqueous solutions, Pamukkale Univ. J. Eng. Sci., 23 (2017) 912–918.
[34] W. Li, K. Yang, J. Peng, L. Zhang, S. Guo, H. Xia, Effects of carbonization temperatures on characteristics of porosity in coconut shell chars and activated carbons derived from carbonized coconut shell chars, Ind. Crops Prod., 28 (2008) 190–198.
[35] P.T. Le, H.T. Bui, D.N. Le, T.H. Nguyen, L.A. Pham, H.N. Nguyen, Q.S. Nguyen, T.P. Nguyen, N.T. Bich, T.T. Duong, M. Herrmann, S. Ouillon, T.P.Q. Le, Preparation and characterization of biochar derived from agricultural by-products for dye removal, Adsorpt. Sci. Technol., 2021 (2021) 9161904, doi: 10.1155/2021/9161904.
[36] F. Bouhamed, Z. Elouear, J. Bouzid, Adsorptive removal of copper(II) from aqueous solutions on activated carbon prepared from Tunisian date stones: equilibrium, kinetics and thermodynamics, J. Taiwan Inst. Chem. Eng., 43 (2012) 741–749.
[37] H. Sayılı, Yeni bir hammaddeden üretilmiş karbonlu malzemenin yapısal, morfolojik ve gözenek özellikleri üzerine çalışmalar, 81 (2017) 245–252.
[38] H. Laksaci, A. Khelifi, M. Trari, A. Addoun, Synthesis and characterization of microporous activated carbon from coffee grounds using potassium hydroxides, J. Cleaner Prod., 147 (2017) 254–262.
[39] M. Kaya, Ö. Şahin, C. Saka, Preparation and TG/DTG, FTIR, SEM, BET surface area, iodine number and Methylene blue number analysis of activated carbon from pistachio shells by chemical activation, Int. J. Chem. Reactor Eng., 16 (2018) 1–13, doi: 10.1515/ijcre-2017-0060.
[40] B. Heibati, S. Rodriguez-Couto, M.A. Al-Ghouti, M. Asif, I. Tyagi, S. Agarwal, V.K. Gupta, Kinetics and thermodynamics of enhanced adsorption of the dye AR 18 using activated carbons prepared from walnut and poplar woods, J. Mol. Liq., 208 (2015) 99–105.
[41] M. Ge, X. Wang, M. Du, G. Liang, G. Hu, S.M. Jahangir Alam, Adsorption analyses of phenol from aqueous solutions using magadiite modified with organo-functional groups: kinetic and equilibrium studies, Materials, 12 (2019) 1–16, doi: 10.3390/ma12010096.
[42] H. Xue, X. Wang, Q. Xu, F. Dhaouadi, L. Sellaoui, M.K. Seliem, A.B. Lamine, H. Belmabrouk, A. Bajahzar, A. Bonilla-Petriciolet, Z. Li, Q. Li, Adsorption of Methylene blue from aqueous solution on activated carbons and composite prepared from an agricultural waste biomass: a comparative study by experimental and advanced modeling analysis, Chem. Eng. J., 430 (2022) 132801, doi: 10.1016/j.cej.2021.132801.
[43] S. Afroze, T. Kanti Sen, H.M. Ang, Adsorption performance of continuous fixed bed column for the removal of Methylene blue (MB) dye using *Eucalyptus sheathiana* bark biomass, Res. Chem. Intermed., 42 (2016) 2343–2364.
[44] A. Medhat, H.H. El-Maghrabi, A. Abdelghany, N.M. Abdel Menem, P. Raynaud, Y.M. Moustafa, M.A. Elsayed, A.A. Nada, Efficiently activated carbons from corn cob for Methylene blue adsorption, Appl. Surf. Sci. Adv., 3 (2021) 100037, doi: 10.1016/j.apsadv.2020.100037.
[45] Y. Liu, Is the free energy change of adsorption correctly calculated?, J. Chem. Eng. Data, 54 (2009) 1981–1985.
[46] J. Saikia, G. Das, Framboidal vaterite for selective adsorption of anionic dyes, J. Environ. Chem. Eng., 2 (2014) 1165–1173.
[47] E. Altıntıg, S. Balta, M. Balta, Z. Aydemır, Methylene blue removal with ZnO coated montmorillonite: thermodynamic, kinetic, isotherm and artificial intelligence studies, Int. J. Phytorem., (2021), doi: 10.1080/15226514.2021.1984386 (in Press).
[48] E. Kavci, Malachite green adsorption onto modified pine cone: isotherms, kinetics and thermodynamics mechanism, Chem. Eng. Commun., 208 (2021) 318–327.
[49] Mu. Naushad, A.A. Alqadami, Z.A. AlOthman, I.H. Alsohaimi, M.S. Algamdi, A.M. Aldawsari, Adsorption kinetics, isotherm and reusability studies for the removal of cationic dye from aqueous medium using arginine modified activated carbon, J. Mol. Liq., 293 (2019) 111442, doi: 10.1016/j.molliq.2019.111442.
[50] G. Sharma, B. Thakur, A. Kumar, S. Sharma, Mu. Naushad, F.J. Stadler, Atrazine removal using chitin-*cl*-poly(acrylamide-*co*-itaconic acid) nanohydrogel: Isotherms and pH responsive nature, Carbohydr. Polym., 241 (2020) 116528, doi: 10.1016/j.carbpol.2020.116258.
[51] A.K. Agarwal, M.S. Kadu, C.P. Pandhurnekar, I.L. Muthreja, Langmuir, Freundlich and BET adsorption isotherm studies for zinc ions onto coal fly ash, Int. J. Application Innovation Eng. Manage., 3 (2014) 64–71.
[52] O. Pezoti, A.L. Cazetta, K.C. Bedin, L.S. Souza, R.P. Souza, S.R. Melo, V.C. Almeida, Percolation as new method of preparation of modified biosorbents for pollutants removal, Chem. Eng. J., 283 (2016) 1305–1314.
[53] H. Shayesteh, A. Ashrafi, A.R. Kelisham, Evaluation of Fe_3O_4@MnO_2 core-shell magnetic nanoparticles as an adsorbent for decolorization of Methylene blue dye in contaminated water: synthesis and characterization, kinetic, equilibrium, and thermodynamic studies, J. Mol. Struct., 1149 (2017) 199–205, doi: 10.1016/j.molstruc.2017.07.100.
[54] M. Kilic, E. Apaydin-Varol, A.E. Pütün, Adsorptive removal of phenol from aqueous solutions on activated carbon prepared from tobacco residues: equilibrium, kinetics and thermodynamics, J. Hazard. Mater., 189 (2011) 397–403.
[55] H. Demiral, G. Gündüzoğlu, Removal of nitrate from aqueous solutions by activated carbon prepared from sugar beet bagasse, Bioresour. Technol., 101 (2010) 1675–1680.
[56] A. Vimalkumar, J. Thilagan, K. Rajasekaran, C. Raja, M.N. Flora, Preparation of activated carbon from mixed peels of fruits with chemical activation (K_2CO_3) – application in adsorptive removal of Methylene blue from aqueous solution, Int. J. Environ. Waste Manage., 22 (2018) 260–271.
[57] T.M. Dao, T. Le Luu, Synthesis of activated carbon from macadamia nutshells activated by H_2SO_4 and K_2CO_3 for Methylene blue removal in water, Bioresour. Technol. Rep., 12 (2020) 100583, doi: 10.1016/j.biteb.2020.100583.
[58] P. Nowicki, A. Bazan, J. Kazmierczak-Razna, R. Pietrzak, Sorption properties of carbonaceous adsorbents obtained by pyrolysis and activation of pistachio nut shells, Adsorpt. Sci. Technol., 33 (2015) 581–586.
[59] R.H. Khuluk, A. Rahmat, Buhani, Suharso, Removal of Methylene blue by adsorption onto activated carbon from coconut shell (*Cocos nucifera* L.), Indones. J. Sci. Technol., 4 (2019) 229–240.
[60] F. Marrakchi, B.H. Hameed, M. Bouaziz, Mesoporous and high-surface-area activated carbon from defatted olive cake by-products of olive mills for the adsorption kinetics and isotherm of Methylene blue and acid blue 29, J. Environ. Chem. Eng., 8 (2020) 104199, doi: 10.1016/j.jece.2020.104199.
[61] J. Yener, T. Kopac, G. Dogu,T. Dogu, Batch adsorber rate analysis of Methylene blue on amberlite and clinoptilolite, Sep. Sci. Technol., 41 (2006) 1857–1879.